Advancements in GaN-based Horizontal-Cavity and Surface-Emitting Superluminescent Diodes for Next Generation Holographic Displays

Muhammet Genc*[1], Zhi Li[1], Juan S. D. Morales[1], Abhinandan Hazarika[1], HowYuan Hwang[1], Kaan Aksit[2], Gerry O'Carroll[1], Brendan Roycroft[1], Brian Corbett[1]

[1]Tyndall National Institute, University College Cork, Lee Maltings, T12 R5CP Cork, Ireland
[2]Department of Computer Science, University College London, London, UK

ABSTRACT

Surface-emitting superluminescent diodes (SLDs) with horizontal cavities in the visible spectrum offer a significant advancement in optoelectronics, combining the benefits of LEDs and laser diodes. Characterized by broad emission spectrum, directionality, and high output power, SLDs are ideal for applications requiring high-brightness, high spatial coherence, and low temporal coherence, such as imaging and projection systems due to their speckle-free emission. This study focuses on SLDs emitting in the blue spectral region using gallium nitride (GaN) materials. Advanced fabrication techniques yielded a surface-emitting architecture using horizontal ridge waveguiding with a 45° total internal reflector on the facets, achieving high power and broad spectral output. The SLDs demonstrated a peak emission wavelength in the 4xx nm range with FWHM of 2-8 nm, depending on cavity length, and peak optical output power up to 1 W under pulse conditions. These features make SLDs cost-effective and suitable for next-gen optical systems, including holographic display applications, highlighting their potential for widespread adoption in high-performance technologies.

Keywords: Surface emission, superluminescence, speckle-free light, cost effective, high power, holography, AR/VR

1. INTRODUCTION

The demand for efficient, high-power light emitters with low etendue, broad spectra, and minimal speckle is increasingly critical in advanced display, spectroscopy, and measurement applications. Lasers are well-suited for such applications due to their high power and low etendue, but their high temporal coherence leads to undesirable speckle patterns. On the other hand, light-emitting diodes (LEDs) offer broad spectral emission and high efficiency but struggle with low coupling efficiency, particularly when used with small areas and low numerical apertures. SLDs combine the beneficial characteristics of both LEDs and laser diodes (LDs), offering high brightness, broad emission spectra, and reduced temporal coherence. These properties make SLDs ideal for applications requiring high spatial coherence and speckle-free light emission, such as imaging, projection, and sensing systems. Unlike LDs, which exhibit narrow spectral linewidths and high temporal coherence, SLDs provide a broader spectral output with lower temporal coherence, minimizing speckle patterns that can degrade the performance of holographic and imaging systems.

A key characteristic of SLDs is their ability to generate amplified spontaneous emission (ASE) without the optical feedback typically found in lasers [1]. This occurs when the carrier density in a longitudinal waveguide is high enough to induce ASE, while feedback is suppressed, resulting in light emission with the spatial coherence of the waveguide and the broad spectral content of the gain spectrum. This behavior is governed by an exponential dependence on the carrier and current density, modal gain spectrum, waveguide loss, and waveguide length, as described by the relationship:

$$P = P_{sp} \exp\big(\Gamma g(N,\lambda) - \alpha(N,\lambda)\big) L$$

Where P_{sp} represents the initial spontaneous emission power, $\Gamma g(N,\lambda)$ is the modal gain spectrum as a function of carrier density, N, and wavelength, λ; $\alpha(N,\lambda)$ denotes the waveguide losses, and L is the waveguide length. The exponential factor captures the balance between gain and loss, determining the total emitted power. Here, P_{sp} includes a spontaneous coupling factor, typically around 10^{-3}, much higher than that of lasers due to the broad spontaneous emission spectrum. At high current densities, the power conversion efficiency of SLDs can be comparable to that of lasers and much higher than that of LEDs, enabling superior performance for various optoelectronic applications.

In this study, we explore the design and performance of GaN-based surface-emitting SLDs operating in the blue spectral region. GaN, with its wide bandgap of 3.4 eV, is an ideal material for efficient blue light emission, which is particularly crucial for high-resolution holographic displays. Blue light contributes to fine pixel resolution and overall brightness, making GaN-based SLDs a promising solution for next-generation holographic displays, which demand coherent light sources that emit over a broad spectral range while minimizing temporal coherence to reduce speckle and interference patterns. The development of GaN-based surface-emitting SLDs represents a significant advancement in meeting the challenging requirements of modern display and sensing technologies, bridging the gap between LEDs and laser diodes in terms of both performance and application versatility [2].

2. DEVICE DESIGN AND FABRICATION

2.1 Epitaxial Structure

The GaN-based SLDs were grown on low defect density free-standing GaN substrates using metalorganic chemical vapor deposition (MOCVD), the standard method for high-quality GaN growth. The epitaxial structure was optimized to maximize carrier injection and recombination efficiency. The active region consists of multiple quantum wells (MQWs) designed for efficient blue emission, with the well widths tailored to achieve peak emission at around 4xx nm. The structure includes a 1 µm thick n-type AlGaN bottom cladding layer, an active region of two InGaN quantum wells (QWs) separated by GaN barriers, and an Mg-doped AlGaN electron blocking layer. Above the active region, a 120 nm thick p-type GaN waveguide layer is followed by a 500 nm thick p-type AlGaN cladding layer, and the structure is completed with a p-doped GaN cap layer. This structure allows for high current injection and effective radiative recombination, which is crucial for achieving high optical output power.

2.2 Surface-Emitting Architecture with Ridge Waveguide and TIR Facet Reflectors

A surface-emitting configuration was chosen for the devices, leveraging a ridge waveguide structure to confine the optical mode in the lateral direction. The ridge waveguide is key to ensuring that the emitted light is efficiently guided and confined, maximizing the emission efficiency. The waveguide design was optimized for blue light, with dimensions that balance optical confinement and efficient carrier injection. A critical feature of the surface-emitting SLD design is the inclusion of a 45° total internal reflector (TIR) on the device facets [2]. This reflector serves to redirect the emitted light outward, significantly improving the directionality of the emission and minimizing the light lost to scattering. The 45° angle is selected to optimize internal reflection and enhance the coupling of light into the far-field, which is particularly important for applications in projection and holographic displays.

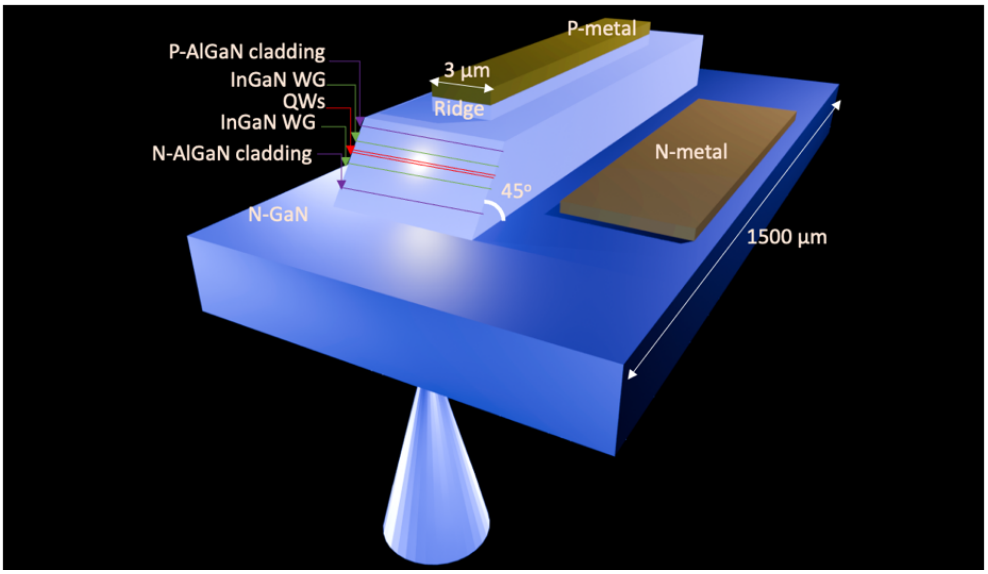

Figure 1. 3D schematic of single beam SLD design.

Ridge waveguides with a width of 3 µm and a gain lengths of 700 µm, 1000 µm and 1500 µm were fabricated by etching the top surface of the active region. For the p-type contact, a Pd/Ni/Au metal alloy was employed, followed by an annealing process to ensure proper contact formation. For the n-type contact, a Ti/Al/Ti/Au metallization scheme was utilized. A SiO_2 layer was subsequently sputtered over the entire wafer surface, and selective oxide etching was performed to expose the p- and n-type contact regions. Bond pads were then formed by depositing Ti/Pt/Au on the exposed contact areas.

To define the substrate-emitting device geometry, two 45° angled facets were etched to a depth of 2.7 µm, which acted as total internal reflection (TIR) turning mirrors. A second SLD geometry with one 45º output mirror (Fig.1) was configured where the second facet was vertically etched to create 90º mirror using an Inductively Coupled Plasma (ICP) process. The mirror was then coated with SiO_2 and Al layers to achieve high reflectivity (HR) coating. The transparent GaN substrate was polished to reduce light scattering, enhancing optical performance. Finally, to improve light extraction and minimize feedback, a SiO_2 antireflective (AR) coating was applied to the bottom surface of the wafer (Fig. 2a, b, c, d). The devices, being surface-emitting, provide a cost-effective approach for on-wafer measurement. After characterizing the devices, the wafer was diced to isolate individual emitters. Following the dicing process, each emitter was flip-chip bonded onto an aluminum nitride (AlN) submount. The submount was then positioned within a TO-5 package, after which wire bonding was performed to establish electrical connections (Fig. 2e).

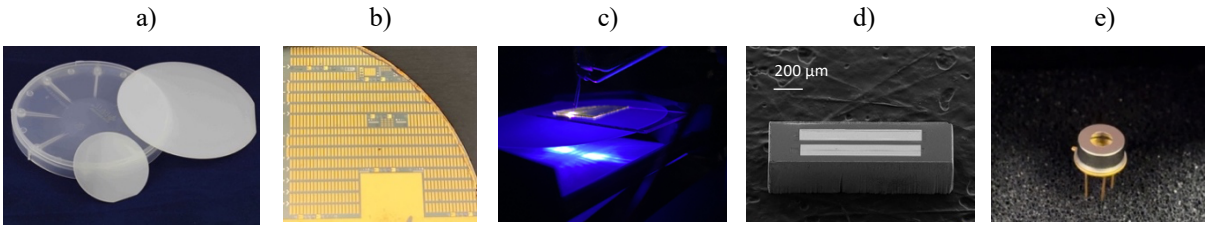

Figure 2. Fabrication cycle of SLDs. a) GaN epitaxial wafer. b) Fabricated SLDs on-wafer. c) On-wafer testing. d) Single SLD emitter. e) Packaged (TO-5) SLD.

To characterize the angle of the etched facets, several advanced techniques were employed, including scanning electron microscopy (SEM) (Fig. 3a), focused ion beam (FIB) milling, mechanical scanning, and atomic force microscopy (AFM). While SEM and FIB provided initial structural insights, AFM proved to be the most effective method for precise angle measurement due to its high spatial resolution and sensitivity to surface topography (Fig. 3b). Both single-beam and two-beam configurations were investigated, with angles of 90° and 45° for the single-beam, and 45° for both facets in the two-beam configuration. AFM imaging revealed that the etched mirror facets closely adhered to the designed angles, with minimal surface roughness and deviations. This comprehensive analysis confirmed the high accuracy of the ICP etching process and demonstrated the efficacy of AFM in providing reliable angular measurements, essential for optimizing the device's light emission and overall optical performance.

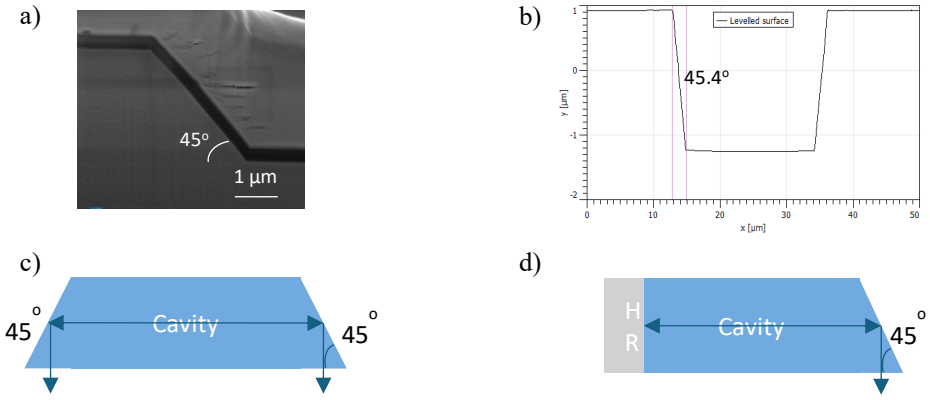

Figure 3. a) SEM image of 45-degree mirror in GaN. b) AFM scan profile from mirror. c) Two output beam configurations with two 45-degree mirrors on both facets. d) Single output beam configuration with one 45-degree mirror.

3. RESULTS AND DISCUSSION

3.1 Optical Characteristics and Spectral Performance

The GaN-based SLDs exhibited peak emission wavelengths around 4xx nm, with a full-width at half maximum (FWHM) of the emission spectrum ranging from 2 to 8 nm depending on the cavity length and drive current. Devices with shorter cavity lengths (e.g., 700 µm) exhibited broader emission spectra, while those with longer cavities (e.g., 1500 µm) showed narrower spectra, which is typical for superluminescent behavior. The broader spectrum is advantageous for reducing speckle and interference in holographic applications, where the goal is to provide a smooth, continuous wavefront without the interference fringes common in laser-based systems.

Figures 4a and 4b illustrate the intensity distribution of the emission in the far field. The two and one intensity peaks correspond to the emission from the two and one turning mirrors, respectively. The divergence angles of approximately 10° and 20° for the individual output modes are determined from the FWHM of the intensity as a function of angle for each peak. The greater divergence observed in the longitudinal direction can be attributed to the tight confinement of the mode within the transverse waveguide.

In the context of computer-generated holography (CGH), the far-field intensity distribution is crucial for understanding how the light will propagate and interact with holographic elements. The divergence angles provide key information that helps in optimizing the design of the holographic system, ensuring the desired reconstruction quality. Specifically, the higher divergence in the longitudinal direction, resulting from the tight mode confinement, allows for more precise control over the propagation of the beam, which is essential for achieving high-resolution and accurate holographic projections. This far-field data plays a vital role in ensuring that the reconstructed wavefront meets the specifications required for high-fidelity and sharp holographic images.

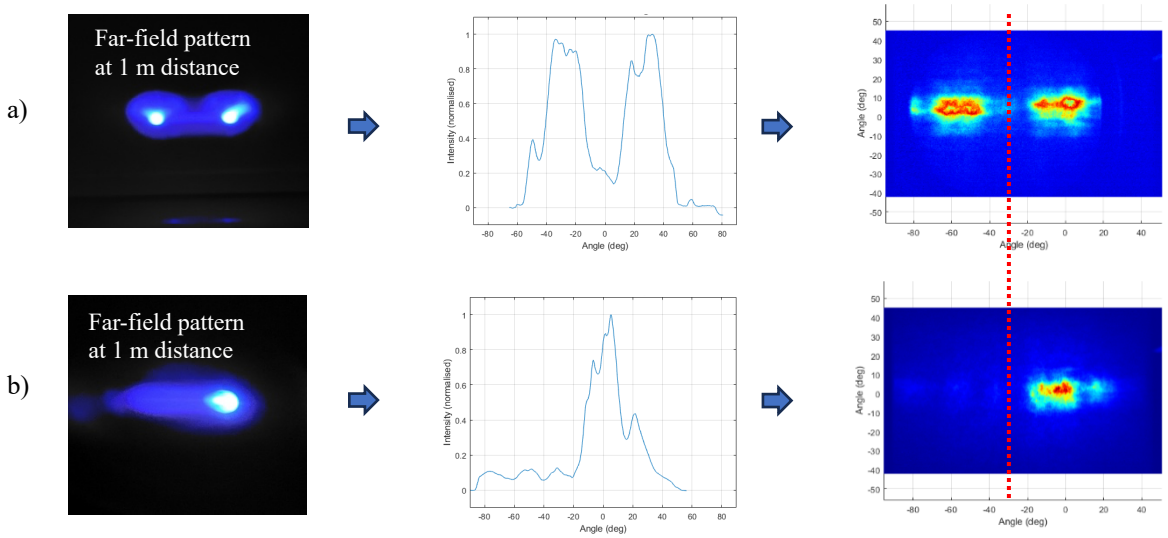

Figure 4. Far field patterns with collimation optics at 1 meter distance and far field divergences. a) Two output beam configuration. b) Single output beam configuration.

A peak optical power of 1 W was achieved under pulsed conditions (300 ns pulse width, 10 kHz repetition rate) at a drive current of 1.6 A, with a corresponding voltage of approximately 8 V (Figure 5a). The spectral profile, measured at various current levels, revealed a FWHM of 7.5 nm at 400 mA and 4.2 nm at 1 A, with measurements obtained from GaN Wafer (A) under the same pulsed operating conditions (Figure 5b).

Under identical pulsed conditions, a peak optical power of 175 mW was observed at 1.6 A, with the voltage measured between 10–11 V (Figure 5c). Spectral measurements at different current levels showed a FWHM of 7.1 nm at 800 mA and 3.4 nm at 1.6 A (Figure 5d), with these data collected from GaN Wafer (B). The reduction in FWHM with increasing current can be attributed to the higher carrier density and more efficient recombination process at elevated currents, which results in a narrower emission spectrum. The increased current promotes a more uniform carrier distribution, reducing

inhomogeneous broadening and enhancing recombination efficiency. The devices were capable of operating at pulse durations up to 1 µs without having a heat sink or thermoelectric cooler (TEC). However, for pulse durations exceeding 1 µs, the implementation of a heat sink and TEC controller becomes necessary to manage the increased thermal load. For pulse lengths beyond 1 µs, thermal effects induce significant heating, which leads to spectral broadening. As the temperature rises, the emission characteristics of the device shift, eventually transitioning from superluminescence to behavior resembling that of a light-emitting diode (LED), with a broader and less coherent spectrum. This transition is driven by the increased carrier recombination at higher temperatures, resulting in reduced efficiency and a more thermally dominated emission.

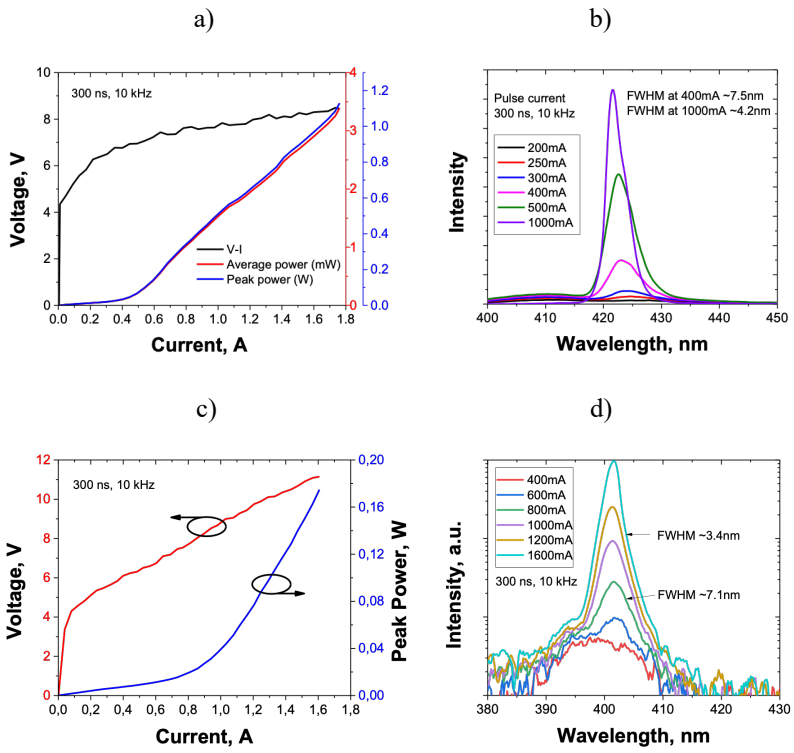

Figure 5. a) L-I-V characteristic of SLD under pulse conditions from Wafer (A). b) Spectrum profile under different current levels from wafer (A). c) L-I-V characteristic of SLD under pulse conditions from Wafer (B). d) Spectrum profile under different current levels from wafer (B).

The spectral characteristics of SLDs with different cavity lengths (700 µm, 1000 µm, and 1500 µm) and a constant ridge width of 3 µm were investigated under pulsed injection conditions (300 ns pulse width, 10 kHz repetition rate, and 800 mA pulse current).

The measured FWHM of the emission spectra showed a clear dependence on cavity length, with the 700 µm cavity exhibiting a FWHM of 8.4 nm, the 1000 µm cavity a FWHM of 5.1 nm, and the 1500 µm cavity the narrowest spectrum at 4.2 nm (Fig. 6a, b, c). This reduction in spectral width with increasing cavity length is attributed to a decrease in the number of supported longitudinal modes, leading to more coherent emission and narrower spectral output. Longer cavities support fewer modes, reducing mode competition and spectral broadening, which results in a sharper emission profile. This narrowing of the spectrum is particularly beneficial for computer-generated holography (CGH) applications in augmented reality (AR) and virtual reality (VR), where high spatial coherence and narrow spectral linewidths are critical for achieving high-resolution, realistic holographic projections.

Additionally, the impact of pulse conditions on the spectral properties highlights the importance of heat management in high-power diode operation. At 800 mA pulse current, thermal effects can influence both the spectral properties and device performance, with shorter cavity lengths potentially suffering from increased thermal buildup due to higher mode competition and carrier injection inefficiencies. Longer cavities, on the other hand, may provide more efficient heat dissipation and more stable operating conditions, which is crucial for maintaining performance in AR/VR systems that demand high precision and low thermal distortion.

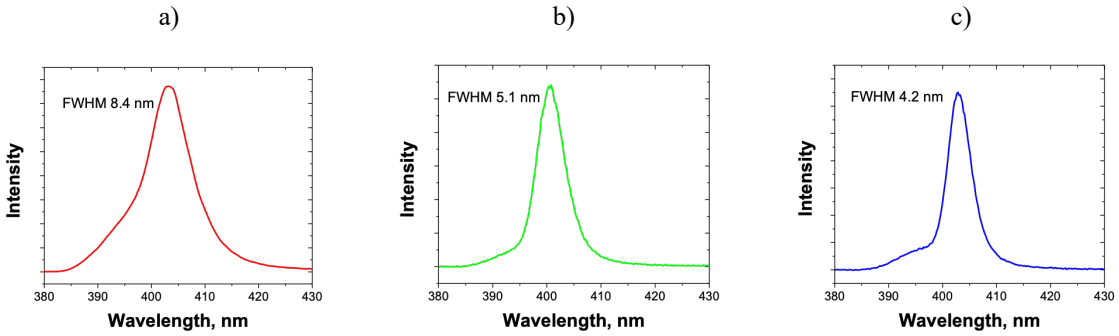

Figure 6. Cavity length-dependent spectrum at 800 mA current (300 ns pulse width, 10 kHz repetition rate) for devices with lengths of: a) 700 µm, b) 1000 µm, c) 1500 µm.

3.2 Speckle-Free Emission, Temporal and Spatial Coherence

The GaN-based SLDs exhibit key characteristics that make them highly suitable for CGH applications, notably their speckle-free emission. Due to their broad spectral output and low temporal coherence, these devices minimize unwanted interference patterns like speckle, a common issue in laser-based systems. The coherence length Lc, which is inversely proportional to the spectral width, is given by the formula:

$$Lc=\lambda^2/\Delta\lambda$$

where λ is the central wavelength and $\Delta\lambda$ is the spectral width (FWHM). For a central wavelength of 405 nm, the coherence length is calculated as 19.58 µm, 32.18 µm and 39.05 µm for spectral widths of 8.4 nm, 5.1 nm, and 4.2 nm, respectively. This indicates a short coherence length, which is critical for reducing temporal coherence and minimizing speckle in dynamic holographic systems. The reduced temporal coherence is crucial for multi-dimensional holographic displays, where temporal coherence can limit image stability and quality.

The spatial coherence is high due to the narrow far-field divergence angle, meaning that the light maintains a fixed phase relationship across the beam's cross-section. This is essential for holography, where maintaining phase coherence over large volumes without creating interference patterns is required. The spatial coherence ensures that the light beam remains collimated over long distances, preventing distortion and interference. These combined properties reduced temporal coherence, short coherence length, and high spatial coherence make the GaN-based SLDs ideal for CGH, enabling stable, high-quality, and speckle-free images in holographic displays.

3.3 Device Long-Term Stability

The performance of GaN-based SLDs, characterized under both CW and pulsed conditions, shows promising potential for CGH applications. Current-voltage (I-V) measurements under CW conditions (Figure 7a) indicate minimal variation across the wafer, reflecting robust material uniformity and reliable device performance, which are critical for large-scale production and consistent operation in practical applications. The SLDs exhibit a current density of 5.5 kA/cm² at 250 mA, demonstrating the device's capability to handle high power injection. This is particularly important for CGH systems that require significant light intensity for generating high-resolution holograms with fine detail and clarity. Under pulsed conditions (Figure 7b), a slight 4.04% power drop was observed over a 2-hour period at a 1 µs pulse width and 10 kHz repetition rate, emphasizing the SLD's ability to maintain a stable output even under high-speed, dynamic switching. This minimal power degradation highlights the robust performance of the SLDs, making them suitable for 3D holographic displays that require real-time image with minimal degradation.

Temperature-dependent wavelength shifts (Figure 7c) show a total 2.45 nm shift from 20°C to 80°C, corresponding to a central wavelength shift of approximately 40.83 pm/K. This temperature-induced shift is consistent with the behavior of GaN-based lasers, where the emission wavelength increases with rising temperature due to bandgap narrowing. Although this shift is relatively small, it may still affect the accuracy of holograms in CGH applications, where wavelength stability is crucial for precise interference patterns. Such shifts may require temperature compensation techniques to ensure the wavelength remains stable and does not introduce distortion in the generated holographic image. Overall, the low IV variation, stable power output, and manageable temperature-induced wavelength shift make these SLDs highly suitable for CGH systems. However, effective thermal management remains essential to optimize performance under varying environmental conditions, ensuring consistent image quality and performance in next-generation holographic displays.

The ability of these devices to deliver high output power, with minimal degradation, and with a manageable temperature response positions them as an ideal solution for high-performance, speckle-free holography.

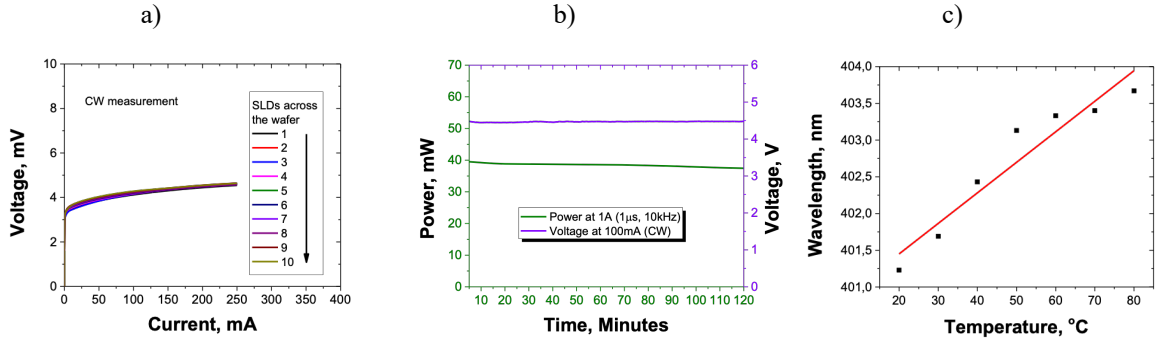

Figure 7. a) I-V characteristics showing uniformity across the wafer. b) Voltage and power stability measured over a 2-hour period, under CW and pulsed conditions (1 µs pulse width, 10 kHz repetition rate). c) Temperature-dependent wavelength shift observed from 20°C to 80°C.

4. IMPLICATIONS FOR HOLOGRAPHIC DISPLAYS

In collaboration with University College London, an original CHG image was utilized (Figure 7a), where a 405 nm SLD served as the light source in the holographic setup shown in Figure 7b, which included a collimating lens, beam splitter, spatial light modulator (SLM), focusing lens, and CCD camera to capture the CHG hologram. The SLD was compared to a commercial 405 nm LD for hologram quality assessment. As shown in Figures 7c and 7d, the SLD produced a hologram with higher contrast and better image quality compared to the LD [3, 4]. This improvement is attributed to the SLD's low temporal coherence and speckle-free emission, which reduce artifacts and interference patterns that typically affect LD-based holograms. The broad spectral output of the SLD limits temporal coherence, thereby minimizing speckle, while its high spatial coherence maintains focus over large distances, essential for sharp holographic images. Additionally, in Figure 7e, the back of the hologram, featuring a steering wheel, displayed enhanced detail and contrast when illuminated by the SLD, highlighting the superior imaging capabilities of the SLD-based system [5].

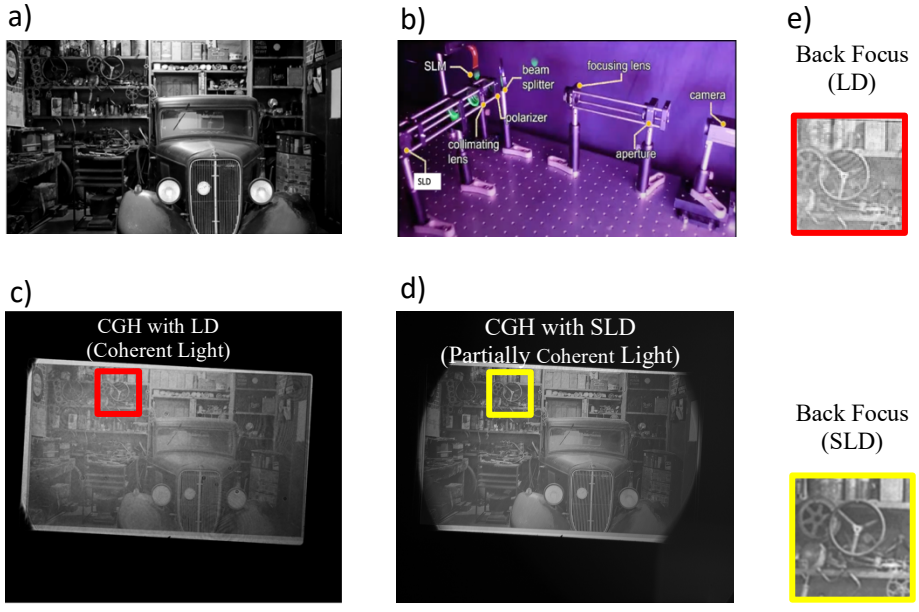

Figure 8. a) Original CHG image used for hologram testing. b) Optical setup for holography. c) Hologram generated using a commercial LD. d) Hologram generated using Tyndall's SLD. e) Hologram images with back focus.

5. CONCLUSION

We have demonstrated GaN-based surface-emitting superluminescent diodes operating in the blue spectral region, suitable for next-generation displays. These devices exhibit high optical output power, broad spectral output, and speckle-free emission, making them an ideal candidate for high-performance holographic display systems. The novel epitaxial structure and advanced surface-emitting architecture, combined with the use of ridge waveguides and total internal reflectors, enable efficient light extraction and high output power. The results highlight the potential of GaN-based SLDs to revolutionize optoelectronic applications, particularly in the field of 3D visualization and holographic displays.

ACKNOWLEDGMENTS

The authors would like to acknowledge Enterprise Ireland Contract No. CF 2023 2115P for their support of this research.

REFERENCES

[1] A. Kafar, S. Stanczyk, M. Sarzynski, S. Grzanka, J. Goss, G. Targowski, A. Nowakowska-Siwinska, T. Suski, and P. Perlin, “Nitride superluminescent diodes with broadened emission spectrum fabricated using laterally patterned substrate,” Opt. Express 24, 9673-9682 (2016).

[2] R. Cahill, P.P. Maaskant, M. Akhter, B. Corbett, “High power surface emitting InGaN superluminescent light-emitting diodes,” Appl. Physics Letters 115, 171102 (2019).

[3] Kavaklı, Koray, Liang Shi, Hakan Urey, Wojciech Matusik, and Kaan Akşit. "Multi-color holograms improve brightness in holographic displays." In SIGGRAPH Asia 2023 Conference Papers, pp. 1-11. (2023).

[4] Zhan, Yicheng, Koray Kavaklı, Hakan Ürey, Qi Sun, and Kaan Akşit. "AutoColor: learned light power control for multi-color holograms." In Optical Architectures for Displays and Sensing in Augmented, Virtual, and Mixed Reality (AR, VR, MR), 12913, pp. 96-102. SPIE, (2024).

[5] Peng Y, Choi S, Kim J, Wetzstein G. Speckle-free holography with partially coherent light sources and camera-in-the-loop calibration. Sci Adv., Nov 12;7(46), (2021).